Molecular Cancer Therapeutics

AACR-NCI-EORTC International Conference
Molecular Targets and Cancer Therapeutics
Discovery, Biology, and Clinical Applications
October 22-26, 2007

AACR Educational Workshops in Singapore:
Pathobiology of Cancer Clinical Trial Design
Application Deadline: Sept. 4, 2007

HOME   HELP   FEEDBACK   SUBSCRIPTIONS   ARCHIVE   SEARCH   TABLE OF CONTENTS

Institution: UNIVERSIDAD DE MALAGA | Sign In via User Name/Password

Research Articles: Therapeutics, Targets, and Development

Loss of mitochondrial membrane potential is inhibited by bombesin in etoposide-induced apoptosis in PC-3 prostate carcinoma cells

Mercedes Salido[1], Juan L. Gonzalez[2] and Jose Vilches[1]

Departments of [1] Histology and [2] Statistics and Operational Research, School of Medicine, University of Cadiz, Cádiz, Spain

Requests for reprints: Mercedes Salido, Laboratory 57, Servicios Centrales de Investigación en Ciencias de la Salud, c/Dr. Marañon 3, 11002 Cádiz, Spain. Phone: 34-95601-5832; Fax: 34-95601-5265. E-mail: mercedes.salido@uca.es

This Article

▸ **Abstract** FREE
▸ **Full Text (PDF)**
▸ **Alert me when this article is cited**
▸ **Alert me if a correction is posted**

Services

▸ **Email this article to a friend**
▸ **Similar articles in this journal**
▸ **Similar articles in PubMed**
▸ **Alert me to new issues of the journal**
▸ **Download to citation manager**

Google Scholar

▸ **Articles by Salido, M.**
▸ **Articles by Vilches, J.**

PubMed

▸ **PubMed Citation**
▸ **Articles by Salido, M.**
▸ **Articles by Vilches, J.**

Abstract

Neuroendocrine secretory products and their interactions with epithelial prostate cells are currently under investigation in order to understand their significance in the pathogenesis, prognosis, and therapy of prostate carcinoma. These neuropeptides have the potential to disrupt the balance between cell death and cell growth in the tumor. Our research was based on the role of bombesin in modulating the mitochondrial membrane potential ($\Delta\psi_m$) in cell death induced by etoposide on PC-3 cells. Cells were cultured and stained with 5,5',6,6'-tetrachloro-1,1',3,3'-tetraethylbenzimidazolylcarbocyanine iodide (JC-1). At low membrane potentials, JC-1 produces a green fluorescence, and at high membrane potentials, it forms "J aggregates" with red fluorescence. Cells were examined in a confocal microscope. For quantitative analyses, regions of interest were selected. The size, number of pixels, and ratios between fluorescence intensity in the red and green channels in each region of interest were calculated. The loss of $\Delta\psi_m$ in etoposide-treated PC-3 cells was prevented by bombesin. The quantitative analysis of JC-1–stained cells revealed a significant decrease in the red (high $\Delta\psi_m$) to green (low $\Delta\psi_m$) ratio in etoposide-treated cells when compared with control cells, which was restored in the presence of bombesin ($P < 0.00001$). The interaction between treatments and area ($P = 0.0002$) was highly significant, and confirms that PC-3 cells keep

their apoptosis machinery, showing an apoptotic volume decrease in response to etoposide. The protection by bombesin occurs by inhibition of apoptosis and maintenance of mitochondrial integrity. New therapeutic protocols and trials need to be developed to test drugs acting through the neutralization of antiapoptotic intracellular pathways mediated by neuroendocrine hormones. [Mol Cancer Ther 2007;6(4):1292–9]

Introduction

Neuroendocrine differentiation in prostatic adenocarcinomas has received increasing attention in recent years as a result of possible implications in prognosis and therapy (1–4). Neuroendocrine secretory products and their interactions with epithelial prostate cells are currently under investigation in order to understand their significance in the pathogenesis, prognosis, and therapy of prostate gland carcinoma (5–8). Recently, we showed that bombesin inhibits etoposide-induced apoptosis in human androgen-independent prostatic cancer cell lines (9); thus, these neuropeptides could disrupt the balance between cell death and cell growth in the tumor.

The most relevant biological interest in apoptosis is the possibility of its modulation, hence, the identification of inductive and protective factors and their mechanisms of action seem to be the most relevant challenges in apoptosis research. The increasing number of studies enforcing the importance of mitochondria in apoptosis signaling, with an increase in complexity, has resulted in a strong debate concerning the exact sequence of mitochondrial events. Mitochondrial dysfunction in apoptosis is related with specific permeabilization of the outer mitochondrial membrane to large molecules including ions that are relevant in the apoptotic process (10). The detection of the mitochondrial permeability transition event provides an early indication of the initiation of cellular apoptosis. This process is typically defined as a collapse in the electrochemical gradient across the mitochondrial membrane, as measured by the change in the mitochondrial membrane potential ($\Delta\psi$). Loss of mitochondrial $\Delta\psi$, indicative of apoptosis, can be detected by a unique fluorescent cationic dye, 5,5',6,6'-tetrachloro-1,1',3,3'-tetraethylbenzimidazolylcarbocyanine iodide, commonly known as JC-1. JC-1 is a cationic dye that exhibits potential-dependent accumulation in mitochondria, indicated by a fluorescence emission shift from green (~525 nm) to red (~590 nm). Consequently, mitochondrial depolarization is indicated by a decrease in the red/green fluorescence intensity ratio. The potential-sensitive color shift is due to the concentration-dependent formation of red fluorescent "J aggregates" (11). Therefore, a careful analysis of the fluorescence ratio detected will allow researchers to make comparative measurements of membrane potential and determine the percentage of mitochondria within a population that responds to an applied stimulus (12–15).

A recent study from our laboratory showed the ability of etoposide to induce alterations in the $\Delta\psi_m$, with the subsequent release of intermembrane space proteins (16, 17). The development of *in vitro* models for an adequate approach to neuroendocrine differentiation of prostatic carcinoma, and its implications in this disease, is imperative. In the present article, our research was based on the role of a representative neuropeptide, bombesin, in modulating the mitochondrial permeability transition alterations of cell death induced by etoposide on PC-3 cells, thus enforcing that the presence of the secretory products from neuroendocrine cells confers antiapoptotic capabilities on nonneuroendocrine cells in the androgen-insensitive prostatic PC-3 cancer cell line. On the other hand, the interaction between neuroendocrine cells and prostatic carcinoma cells is a novel model for

the study of basic mechanisms of apoptosis. In this sense, new therapeutic protocols and trials need to be developed to test drugs acting through the neutralization of antiapoptotic intracellular pathways mediated by neuroendocrine hormones.

Materials and Methods

Cell Culture
Androgen-independent PC-3 cells (American Type Culture Collection, Manassas, VA) were grown in Ham's F12 (Cambrex, Verviers, Belgium) supplemented with 10% fetal bovine serum (Biowhittaker, Verviers, Belgium) and 4% penicillin-streptomycin (Cambrex) in a water-saturated atmosphere of 5% CO_2 until the beginning of the experiments.

Treatment Administration
All experiments were started with unsynchronized exponentially growing cells. Treatment protocols for etoposide-induced apoptosis and inhibition of apoptosis by bombesin have been previously described by us (9, 18–22). Briefly, cells were seeded in glass-bottomed microplates (Willco wells; Amsterdam, the Netherlands) at a density of 200,000 cells per well and the culture medium was changed to 5% fetal bovine serum–supplemented medium, and was exposed to different treatments 48 h later.

Etoposide-Induced Apoptosis. Cells were exposed to 150 µmol/L of etoposide (Sigma, Steinheim, Germany), added from a 2 mmol/L stock solution in DMSO.

Neuropeptide Exposure Inhibited Etoposide-Induced Apoptosis. Cells were exposed to combined treatments with etoposide (as described above) and bombesin (Sigma; 1 nmol/L).

Control Groups. A control group cultured in the standard medium was used in all experiments; positive controls were treated with bombesin (1 nmol/L). Cells were examined after 48 h of exposure to different treatments; at least five experiments were done. Direct examination by phase contrast microscopy was done at the beginning of the experiments.

Growth Kinetics and Cell Viability. Using the 2,3-bis(2-methoxy-4-nitro-5-sulfophenyl)-2H-tetrazolium-5-carboxanilide inner salt viability assay and trypan blue exclusion, with trypan blue in culture media (0.5%), the growth kinetics and cell viabilities were determined. After incubation of cells with trypan blue, nonstained cells were regarded as viable cells, and blue cells were considered nonviable when observed in a hematocytometer. The percentage of viable cells was defined as the number of nonstained cells / total cell number x 100.

2,3-Bis(2-Methoxy-4-Nitro-5-Sulfophenyl)-2H-Tetrazolium-5-Carboxanilide Inner Salt Assay. Briefly, cells were grown in a 96-well flat-bottomed microtiter plate at a final volume of 100 µL culture medium per well, in a humidified atmosphere (37°C and 5% CO_2). After 24 and 48 h, 50 µL of the 2,3-bis(2-methoxy-4-nitro-5-sulfophenyl)-2H-tetrazolium-5-carboxanilide inner salt labeling mixture (Boehringer-Mannheim, Mannheim, Germany) was added to each well. Cells were incubated for 4 h in a humidified atmosphere, and the absorbance of cells was measured using an ELISA reader at a wavelength of 450 to 500 nm.

Characterization of Apoptosis with Light Microscopy and Fluorescence Microscopy

For microscopic quantification of apoptotic cells, cytospin preparations obtained from *in vitro* cell cultures were used. The sample was taken by collecting the supernatant (containing the floating apoptotic cells) followed by trypsinization of the rest of the monolayer (containing healthy cells). Both fractions were combined to reconstitute the total population and then centrifuged at 1,000 rpm for 5 min to get the pellet. Cells were then washed twice in PBS and cytospun by means of cytobuckets at 1,500 rpm for 5 min. Air-dried samples were stained for light microscopy (H&E) and fluorescence microscopy (fluorescent 4',6-diamidino-2-phenylindole).

Cell Staining. For H&E staining, air-dried slides were fixed in 10% formaldehyde and stained in hematoxylin and counterstained with eosin. For fluorescent 4',6-diamidino-2-phenylindole staining, air-dried slides were fixed in methanol at –20°C for 20 min, air-dried, and stained with 4',6-diamidino-2-phenylindole (Serva, Boehringer-Ingelheim, Heidelberg, Germany) at room temperature for 20 min in the dark, and mounted with an antifading medium (*O*-phenylenediamine; Sigma) in glycerol (Merck, Darmstadt, Germany), and preserved at –20°C in the dark until examination, at a fluorescence range between 300 and 400 nm. The percentage of apoptotic cells was defined as the number of apoptotic cells / total cell number x 100. At least 200 cells should be counted for each experiment.

Assessment of Apoptosis by Annexin V

Cells were stained with Annexin V as recommended by the suppliers (Molecular Probes, Leiden, the Netherlands), conjugated with Alexa Fluor 594 for the evaluation of translocation of phosphatidylserine to the outer leaflet of the plasma membrane, and SYTOX Green (Molecular Probes) for nuclear staining, to a final concentration of 1 µmol/L. The SYTOX Green nucleic acid stain is a high-affinity nucleic acid stain that easily penetrates cells with compromised plasma membranes, and yet, will not cross the membranes of live cells. The SYTOX Green/DNA complex has excitation and emission maxima of 504 and 523 nm, respectively. Annexin V conjugated with Alexa Fluor 594 shows excitation and emission maxima of 590 and 617 nm, respectively. Briefly, after discarding the culture medium, cells were washed with cold PBS, and a staining solution with 80 µL of SYTOX Green solution in Annexin binding buffer and 20 µL of Annexin solution were added to a final volume of 100 µL of staining solution per well. Cells were incubated at 18°C to 24°C in the dark for 15 min, and then washed twice with Annexin binding buffer (supplied) prior to fixation for 10 min in 70% methanol and mounting with Vectashield (Vector Laboratories, Burlingame, CA). Cells were examined in an inverted confocal microscope Leica TCS-SL (Leica Microsystems, Barcelona, Spain).

Mitochondrial Permeability Potential

Cells were stained with the cationic dye JC-1 (MitoPT, Immunohistochemistry Technologies, Bloomington, MN), which exhibits potential-dependent accumulation in mitochondria. At low membrane potentials, JC-1 continues to exist as a monomer and produces a green fluorescence (emission at 527 nm). At high membrane potentials or concentrations, JC-1 forms J aggregates (emission at 590 nm) and produces a red fluorescence.

Staining Procedure. Cells were stained as recommended by the suppliers. Briefly, cells were cultured in glass-bottomed Willco wells for the assay, not exceeding a final amount of 10^6 cells/mL, and after discarding the culture medium, 1x MitoPT staining solutions obtained from a 100x stock

was added to the wells (0.5 mL/well). Cells were then incubated at 37°C for 15 min in a CO_2 incubator and, after discarding the medium, was washed twice with 1 to 2 mL of assay buffer warmed to 37°C. The wash was discarded and a drop of assay buffer was added to the wells prior to immediate examination in the inverted confocal microscope (Leica TCS SL), equipped with an HCX PL APO CS 40.0 x 1.25 oil immersion objective, with an incubation system consisting of a cube that completely covers the microscope and allows us to keep cells at 37°C in a controlled atmosphere with a mixed air/CO_2 flow of 4 L/h and 5% CO_2 during image collection and analysis.

Image Collection and Analysis

Images were collected and processed using the imaging software provided by the Leica TCS SL system. All samples were exposed to the laser for a time interval not more than 5 min to avoid photobleaching. JC-1 was excited at 490 nm. The excitation beam splitter selected was a DD 488/543. Emission fluorescence was collected in TRITC (590 nm) and FITC (530 nm) channels simultaneously. The laser was set to the lowest power that was able to produce a fluorescent signal. The maximum voltage of photomultipliers was used to decrease the required laser power as much as possible, 440.1 V being the lowest and 499 V the highest voltage. A pinhole of 1 Airy unit was used. Images were acquired at a resolution of 1,024 x 1,024, with a voxel size of 247.66 nm.

For quantitative analysis, at least 120 regions of interest were selected in each group (control, etoposide-treated cells, etoposide plus bombesin–treated cells, and bombesin-treated cells) to quantify changes in $\Delta\psi_m$. All of the regions of interest were cells selected under the following criteria: well-defined limits, clear identification of nucleus, and absence of intersection with neighboring cells. The size, number of pixels, and ratios between fluorescence intensity in the red (high membrane potential) and green (low membrane potential) channels in each region of interest were calculated. An increase in the ratio was interpreted as an increase in $\Delta\psi_m$.

Statistical Analysis

The statistical analysis was done with the SPSS program. A two-way ANOVA analysis was used to compare the mean values of the red/green ratios, also introducing the cell size factor of four size groups defined by the quartiles of the distribution of areas. The normality of the groups was contrasted with Kolmogorov-Smirnov test and homogeneity of variances with Cochran's C test. Post hoc contrasts were carried out to detect the differences between groups.

Results

Characterization of the Apoptotic Process

Percentages of Apoptotic Cells. After 48 h of treatment with 100 µg/mL of etoposide, the percentage of apoptotic cells determined according to the examination of H&E, Annexin V, and 4',6-diamidino-2-phenylindole–stained cells was 61.7% in exposed cells and 7.1% in nontreated control cells. In PC-3 cells, the addition of bombesin resulted in a marked decrease of apoptosis (20.43% of apoptotic cells), whereas in the bombesin-treated group, 5.4% of the cells were apoptotic. Annexin V was used to confirm the induction of apoptosis using a confocal microscope.

Growth Kinetics and Cell Viability. All etoposide-treated groups presented worse viability than the control groups. The addition of neuropeptides resulted, as expected, in an increase in cell viability.

$\Delta\psi_m$ **Assessment by Confocal Microscopy.** Control cells showed heterogeneous staining of the cytoplasm with both red and green fluorescence coexisting in the same cell (Fig. 1A). Consistent with a mitochondrial localization, the red fluorescence was mostly found in rod-shaped and granular structures distributed throughout the cytoplasm. Although a minority of the mitochondria exhibited only green fluorescence; these were most conspicuous in areas of cytoplasm surrounding the nucleus. Treatment of PC-3 cells with bombesin increased the red fluorescence and frequent clusters of mitochondria were seen (Fig. 1B). Exposure of PC-3 cells to etoposide induced marked changes in $\Delta\psi_m$ as evident from the disappearance of red fluorescence or the increase of green fluorescence in most cells, with a predominantly peripheral distribution. Some cells were devoid of red fluorescence, which is an indication of the loss of $\Delta\psi_m$ and the severity of cell damage (Fig. 1C). Cell treatment with etoposide plus bombesin increased the red fluorescence in most cells, and protected cells which presented a similar distribution pattern to that observed in the control group, from the loss of $\Delta\psi_m$ (Fig. 1D).
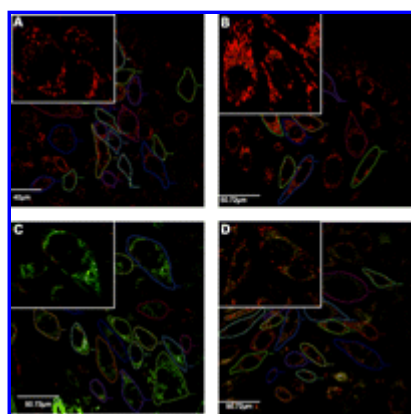

Figure 1. JC-1 fluorescence imaging of mitochondria in the selected regions of interest. *Insets,* a higher magnification of cells (*left*). Cells were stained with JC-1 for 15 min. *Green fluorescence,* depolarized (monomer) mitochondria; *red fluorescence,* hyperpolarized (J aggregates) mitochondria. **A,** control; **B,** bombesin-treated cells; **C,** etoposide-treated cells; **D,** etoposide plus bombesin–treated cells.
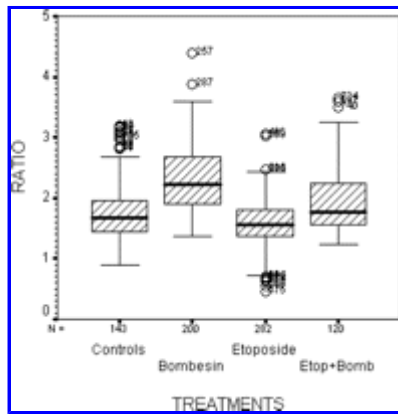
View larger version (57K):
[in this window]
[in a new window]

Statistical Analysis

Descriptive Analysis. For the variable ratio, which is equivalent to the quotient between the mean values of red and green pixels in each region of interest that corresponds to the variable cell area, significant differences ($P < 0.00001$) between the four groups were found (Fig. 2).

Figure 2. Quantification of $\Delta\psi_m$ (box-whisker plot) expressed as a ratio (J aggregates/monomer) in the different treatment groups. Descriptive variables: *X*-axis, *N* for each treatment group; *Y*-axis, red to green ratio.

View larger version (15K):
[in this window]
[in a new window]

Two-Way ANOVA. Using the quartiles of the variable area, four groups were established in the selected cells as a second factor was added which could affect the treatment, with a total of 16 groups, four defined by treatment and four defined by the areas, with four levels per group. Area influence on the red/green ratio between the four treatment groups, treatment influence on the red/green ratio related to area, and the red/green ratio differences depending on the cell area were assessed by means of a two-way ANOVA.

The ANOVA revealed a highly significant difference between the means of ratios between treatments ($P = 0.000$), and the means of ratio for the area sizes ($P = 0.000$), and the interaction between treatments and area ($P = 0.0002$) was also highly significant, indicating that the differences between ratios of the area depend on the treatment. The assumptions of normality of the distribution in the 16 groups were satisfied (except for one group) and the Cochran's C test for homogeneity of variance reported a significance level of >0.05 ($P = 0.12$), that is, we accept that the variances were not significantly different (Fig. 3). This is a strong interaction effect and is unlikely to be due to chance, as shown by ANOVA analysis. Post hoc contrasts were done for confirmation of the significance.
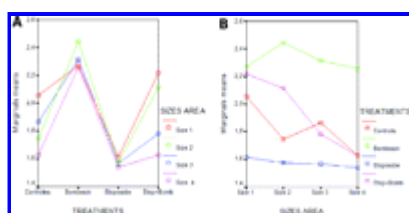

View larger version (16K):
[in this window]
[in a new window]

Figure 3. Profiles of the ratio for marginal means of size for treatment factor (**A**), treatment groups in the *X*-axis and red to green ratio in the *Y*-axis; and for marginal means for size factor (**B**), data for size in the *X*-axis and for red to green ratio in the *Y*-axis.

Post hoc Comparisons. The post hoc comparisons show the differences in model-predicted means for each pair of factor levels. In this case, because the interaction effect was significant, the

differences between the different levels of treatment factor for each of the levels of the factor size were examined to contrast and estimate significant differences between the different treatments conditioned by the factor size. Due to the existence of a control group, the Dunnett test was used (Table 1). Furthermore, the HSD test of Tukey was used to contrast the pairwise differences between treatments (Table 2).

View this table:
[in this window]
[in a new window]
Table 1. Differences between each treatment group and control group with 95% confidence interval showing the influence of size

View this table:
[in this window]
[in a new window]
Table 2. Pairwise differences between the four groups with 95% confidence interval

Discussion

The presence of neuroendocrine differentiation—understood as an exaggerated ratio of neuroendocrine cells to neoplastic epithelial cells in the prostate carcinoma—is associated with worse prognosis, higher tumor progression, and the androgen-independent status of the tumor, which becomes unresponsive to hormonal therapy, and has received increasing attention in recent years as a possible result of implications of therapy (1–4).

The putative function of neuroendocrine cells in stimulating proliferation and/or inhibiting the apoptotic process, worsening the prostate cancer outcome through a paracrine hormonal mechanism, provides a rationale for the experimental use of drugs which could inhibit the secretion of neuroendocrine products, the aim of which is to counteract tumor progression (6–8, 23–25). In the present article, our research was based on the role of bombesin in modulating the induction of mitochondrial membrane potential alterations in etoposide-induced cell death in an androgen-independent PC-3 prostate cancer cell line.

In apoptosis, mitochondria have two essential functions. First, to provide energy in the form of ATP, which is required for cells to die by the apoptotic pathway. Second, to release proapoptotic proteins normally sequestered in the intermembrane space into the cytosol, in which they trigger downstream apoptotic signaling pathways (26–30).

Detection of the mitochondrial permeability transition event provides an early indication of the initiation of cellular apoptosis. This process is typically defined as a collapse in the electrochemical gradient across the mitochondrial membrane, as measured by the change in the mitochondrial $\Delta\psi$. Changes in the mitochondrial $\Delta\psi$ lead to the insertion of proapoptotic proteins into the membrane and possible oligomerization of Bid, Bak, Bax, or Bad. This could create pores, which dissipate the transmembrane potential, thereby releasing cytochrome c into the cytoplasm (31–34).

Loss of mitochondrial $\Delta\psi$, indicative of apoptosis, can be detected with JC-1. JC-1 was incorporated (for easy penetration) into cells and healthy mitochondria, in which it aggregates and fluoresces red (590 nm). When the mitochondrial $\Delta\psi$ collapses in apoptotic cells, the reagent no longer accumulates inside the mitochondria, and instead, it is distributed throughout the cell. When dispersed in this manner, it assumes a monomeric form which fluoresces green (527 nm; refs. 11, 35–37).

A loss of $\Delta\psi_m$ leads to the induction of apoptosis in etoposide-treated PC-3 cells and this damage is prevented by bombesin. The quantitative analysis of JC-1–stained cells revealed a significant decrease in the red (high $\Delta\psi_m$) to green (low $\Delta\psi_m$) ratio in etoposide-treated cells compared with control cells, which was restored in the presence of bombesin. In bombesin-treated cells, an increase in the ratio was observed. Signal transduction molecules activated by bombesin include phosphoinositide-3-kinase/Akt, with subsequent activation of transcription factors (38, 39), whereas the Akt pathway has been involved in the regulation of $\Delta\psi_m$ as well as of cell size (40).

The interaction between treatments and area ($P = 0.0002$), indicating that the difference between ratios of area depends on treatment, is highly significant. Data obtained for etoposide-treated cells confirm that PC-3 cells keep their apoptotic machinery, showing an apoptotic volume decrease in response to etoposide (41). The channel activation leads to a significant decrease in potassium content, and a significant increase in sodium (42–44). The variation in cellular volume was evaluated using the sum of the sodium and potassium contents (45). In previous studies, we have shown that etoposide-treated cells passed through a series of morphologically identifiable stages in their pathway to death. A progressive decrease of intracellular potassium, as cells progress through the different stages, with a dramatic lowering in the final stage (20, 22).

Combined treatment with etoposide and bombesin resulted in a modulation of the apoptotic response with a decrease in apoptosis, and an increase in cell viability even with respect to control cells. The differences in treatment factors vary for each size group. Clear differences were found for size 1 cells between bombesin-treated cells, etoposide plus bombesin–treated cells, and control cells with respect to etoposide-treated cells. For size 2 cells, differences were found between bombesin- and etoposide plus bombesin–treated cells with respect to control and etoposide-treated cells. For sizes 3 and 4, bombesin-treated cells showed a higher ratio than cells in the other three groups. The differences between treatments were remarkable in the control and etoposide plus bombesin–treated cells, but not in etoposide-treated cells and cells exposed to bombesin alone. If there were no interaction effects, the lines in the figures would be parallel. This is a positive fact which confirms the experimental design, and that these data support the role of bombesin as a growing factor (46, 47). The protection by bombesin against etoposide-induced loss of $\Delta\psi_m$, as shown in this study, occurs by the inhibition of apoptosis and maintenance of mitochondrial integrity.

Our evidence shows that the presence of neuroendocrine cells and their secretory products confers antiapoptotic capabilities on nonneuroendocrine cells in androgen-insensitive prostatic cancer cells. New therapeutic protocols and trials need to be developed to test drugs acting through the neutralization of antiapoptotic intracellular pathways mediated by neuroendocrine hormones. Hopefully, this will lead to the development of entirely new therapeutic approaches in hormone refractory prostate cancer.

Footnotes

The costs of publication of this article were defrayed in part by the payment of page charges. This article must therefore be hereby marked *advertisement* in accordance with 18 U.S.C. Section 1734 solely to indicate this fact.

References

1. Vashchenko N, Abrahamsson PA. Neuroendocrine differentiation in prostate cancer: implications for new treatment modalities. Eur Urol 2005;47:147–55.[CrossRef][Medline]
2. Quek ML, Daneshmand S, Rodrigo S, et al. Prognostic significance of neuroendocrine expression in lymph node-positive prostate cancer. Urology 2006;67:1247–52.[CrossRef][Medline]
3. Sciarra A, Cardi A, Dattilo C, Mariotti G, Di Monaco F, Di Silverio F. New perspective in the management of neuroendocrine differentiation in prostate adenocarcinoma. Int J Clin Pract 2006;60:462–70.[CrossRef][Medline]
4. Slovin SF. Neuroendocrine differentiation in prostate cancer: a sheep in wolf's clothing? Nat Clin Pract Urol 2006;3:138–44.[Medline]
5. Wilson EM, Oh Y, Hwa V, Rosenfeld RG. Interaction of IGF-binding protein-related protein 1 with a novel protein, neuroendocrine differentiation factor, results in neuroendocrine differentiation of prostate cancer cells. J Clin Endocrinol Metab 2001;86:4504–11. [Abstract/Free Full Text]
6. Mosca A, Berruti A, Russo L, Torta M, Dogliotti L. The neuroendocrine phenotype in prostate cancer: basic and clinical aspects. J Endocrinol Invest 2005;28:141–5.[Medline]
7. Cabrespine A, Guy L, Gachon F, Cure H, Chollet P, Bay JO. Circulating chromogranin a and hormone refractory prostate cancer chemotherapy. J Urol 2006;175:1347–52.[CrossRef][Medline]
8. Ranno S, Motta M, Rampello E, Risino C, Bennati E, Malaguarnera M. The chromogranin-A (CgA) in prostate cancer. Arch Gerontol Geriatr 2006;43:117–26.[CrossRef][Medline]
9. Salido M, Vilches J, Lopez A, Roomans GM. Neuropeptides bombesin and calcitonin inhibit apoptosis related elemental changes in prostate cancer cell lines. Cancer 2002;94:368–77. [CrossRef][Medline]
10. Antonsson B. Mitochondria and the Bcl-2 family proteins in apoptosis signaling pathways. Mol Cell Biochem 2004;256/257:141–55.
11. Salvioli S, Ardizzoni A, Franceschi C, Cossarizza A. JC-1, but not $DiOC_6(3)$ or rhodamine 123, is a reliable fluorescent probe to asses $\Delta\psi$ changes in intact cells: implications for studies on mitochondrial functionality during apoptosis. FEBS Lett 1997;411:77–82.[CrossRef][Medline]
12. Follstad BD, Wang DI, Stephanopoulos G. Mitochondrial membrane potential differentiates cells resistant to apoptosis in hybridoma cultures. Eur J Biochem 2000;267:6534–40.[Medline]
13. Xu M, Ashraf M. Melatonin protection against lethal myocyte injury induced by doxorubicin as reflected by effects on mitochondrial membrane potential. J Mol Cell Cardiol 2002;34:75–9.[CrossRef][Medline]
14. Custodio JB, Cardoso CM, Madeira VM, Almeida LM. Mitochondrial permeability transition induced by the anticancer drug etoposide. Toxicol In Vitro 2001;15:265–70.[CrossRef][Medline]
15. Fuller KM, Arriaga EA. Advances in the analysis of single mitochondria. Curr Opin Biotechnol 2003;14:35–41.[CrossRef][Medline]

16. Vilches J, Salido M. Mitochondria and cell death. Histol Histopathol 2005; suppl 1: S58–59.
17. Vilches J, Salido M. Neuropeptides as modulators of apoptosis in prostate cancer. In: Figgins HC, editor. Trends in cell apoptosis research. New York: Nova Publishers, Inc., in press 2007.
18. Salido M, Larran J, Lopez A, Vilches J, Aparicio J. Etoposide sensitivity of human prostatic cancer cell lines PC-3, DU 145 and LNCaP. Histol Histopathol 1999;14:125–34.[Medline]
19. Salido M, Vilches J, Lopez A. Neuropeptides bombesin and calcitonin induce resistance to etoposide induced apoptosis in prostate cancer cell lines. Histol Histopathol 2000;15:729–38. [Medline]
20. Salido M, Vilches J, López A, Roomans GM. X-ray microanalysis of etoposide induced apoptosis in the PC-3 prostatic cancer cell line. Cell Biol Int 2001;25:499–508.[CrossRef] [Medline]
21. Salido M, Vilches J, Roomans GM. Changes in elemental concentrations in LNCaP cells are associated with a protective effect of neuropeptides on etoposide-induced apoptosis. Cell Biol Int 2004;28:397–402.[CrossRef][Medline]
22. Vilches J, Salido M, Fernandez-Segura E, Roomans GM. Neuropeptides, apoptosis and ion changes in prostate cancer. Methods of study and recent developments. Histol Histopathol 2004;19:951–61.[Medline]
23. Shariff AH, Ather MH. Neuroendocrine differentiation in prostate cancer. Urology 2006;68:2–8.[Medline]
24. Yamada Y, Nakamura K, Aoki S, et al. Is neuroendocrine cell differentiation detected using chromogranin A from patients with bone metastatic prostate cancer a prognostic factor for outcome? Oncol Rep 2006;15:1309–13.[Medline]
25. Theodoropoulos VE, Tsigka A, Mihalopoulou A. Evaluation of neuroendocrine staining and androgen receptor expression in incidental prostatic adenocarcinoma: prognostic implications. Urology 2005;66:897–902.[CrossRef][Medline]
26. Lawen A. Apoptosis an introduction. Bioessays 2003;25:888–96.[CrossRef][Medline]
27. Kuznetsov AV, Usson Y, Leverve X, Margreiter R. Subcellular heterogeneity of mitochondrial function and dysfunction: evidence obtained by confocal imaging. Mol Cell Biochem 2004;256–257:359–65.
28. Petronilli V, Penzo D, Scorrano L, Bernardi P, Di Lisa F. The mitochondrial permeability transition, release of cytochrome c and cell death. Correlation with the duration of pore openings *in situ*. J Biol Chem 2001;276:12030–4.[Abstract/Free Full Text]
29. Lim ML, Lum MG, Hansen TM, Roucou X, Nagley P. On the release of cytochrome c from mitochondria during cell death signaling. J Biomed Sci 2002;9:488–506.[Medline]
30. James AM, Murphy MP. How mitochondrial damage affects cell function. J Biomed Sci 2002;9:475–87.[Medline]
31. Robertson JD, Orrenius S. Molecular mechanisms of apoptosis induced by cytotoxic chemicals. Crit Rev Toxicol 2000;30:609–27.[Medline]
32. Bouchier-Hayes L, Lartigue L, Newmeyer D. Mitochondria: pharmacological manipulation of cell death. J Clin Invest 2005;115:2640–7.[Abstract/Free Full Text]
33. Armstrong JS. Mitochondria: a target for cancer therapy. Br J Pharmacol 2006;147:239–48. [CrossRef][Medline]
34. Armstrong JS. Mitochondrial membrane permeabilization: the sine qua non for cell death. Bioessays 2006;28:253–60.[CrossRef][Medline]
35. Mathur A, Hong Y, Kemp BK, Alvarez A, Erusalimsky JD. Evaluation of fluorescent dyes for the detection of mitochondrial membrane potential changes in cultured cardiomyocytes. Cardiovasc Res 2000;46:126–38.[CrossRef][Medline]
36. Dedov VN, Cox GC, Roufogalis BD. Visualisation of mitochondria in living neurons with single and two-photon fluorescence laser microscopy. Micron 2001;32:653–60.[CrossRef] [Medline]
37. Castedo M, Ferri K, Roumier T, Metivier D, Zamzami N, Kroemer G. Quantitation of mitochondrial alterations associated with apoptosis. J Immunol Methods 2002;265:39–47. [CrossRef][Medline]
38. Amorino GP, Parsons SJ. Neuroendocrine cells in prostate cancer. Crit Rev Eukaryot Gene Expr 2004;14:287–300.[CrossRef][Medline]

39. Thomas S, Shah G. Calcitonin induces apoptosis resistance in prostate cancer cell lines against cytotoxic drugs via the Akt/survivin pathway. Cancer Biol Ther 2005;4:1226–33.[Medline]
40. Edinger AL, Thompson CB. Akt maintains cell size and survival by increasing mTOR-dependent nutrient uptake. Mol Biol Cell 2002;13:2276–88.[Abstract/Free Full Text]
41. Maeno E, Ishizaki Y, Kanaseki T, Hazama A, Okada Y. Normotonic cell shrinkage because of disordered volume regulation is an early prerequisite to apoptosis. Proc Natl Acad Sci U S A 2000;97:9487–92.[Abstract/Free Full Text]
42. Panayiotidis MI, Bortner CD, Cidlowski JA. On the mechanism of ionic regulation of apoptosis: would the Na+/K+-ATPase please stand up? Acta Physiol (Oxf) 2006;187:205–15. [CrossRef][Medline]
43. Yurinskaya V, Goryachaya T, Guzhova I, et al. Potassium and sodium balance in U937 cells during apoptosis with and without cell shrinkage. Cell Physiol Biochem 2005;16:155–62. [CrossRef][Medline]
44. Yurinskaya VE, Moshkov AV, Rozanov YM, et al. Thymocyte K+, Na+ and water balance during dexamethasone- and etoposide-induced apoptosis. Cell Physiol Biochem 2005;16:15–22.[CrossRef][Medline]
45. Arrebola F, Zabiti S, Canizares FJ, Cubero MA, Crespo PV, Fernandez-Segura E. Changes in intracellular sodium, chlorine, and potassium concentrations in staurosporine-induced apoptosis. J Cell Physiol 2005;204:500–7.[CrossRef][Medline]
46. Albrecht M, Doroszewicz J, Gillen S, et al. Proliferation of prostate cancer cells and activity of neutral endopeptidase is regulated by bombesin and IL-1ß with IL-1ß acting as a modulator of cellular differentiation. Prostate 2004;58:82–94.[CrossRef][Medline]
47. Xiao D, Chinnappan D, Pestell R, Albanese C, Weber HC. Bombesin regulates cyclin D1 expression through the early growth response protein Egr-1 in prostate cancer cells. Cancer Res 2005;65:9934–42.[Abstract/Free Full Text]

Cancer Epidemiology Biomarkers & Prevention   Molecular Cancer Therapeutics
Molecular Cancer Research   Cell Growth & Differentiation

Cancer Epidemiology Biomarkers & Prevention   Molecular Cancer Therapeutics
Molecular Cancer Research   Cell Growth & Differentiation